Journal of Integrative Agriculture 2026, 25(9): 3814–3828

Available online at ScienceDirect

Journal of Integrative Agriculture

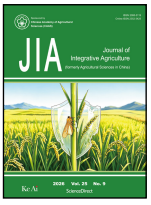

RESEARCH ARTICLE

Dietary sulforaphane modulates hepatic anti-oxidative genes *via* REV-ERBα and histone modifications in pigs

Yiting Wang[1], Shicheng Li[1], Yufei Kan[1], Yanli Zhu[1], Kaiqi Li[1], Haoyu Liu[1, 2], Tadelle Dessie Alemayehu[3], In Ho Kim[4], Mohammad D. Obeidat[5], Rui Zhang[6], Zhaojian Li[1#], Demin Cai[1, 2#]

[1] *Laboratory of Animal Physiology and Molecular Nutrition, Jiangsu Key Laboratory of Animal Genetic Breeding and Molecular Design, College of Animal Science and Technology, Yangzhou University, Yangzhou 225009, China*

[2] *International Joint Research Laboratory in Universities of Jiangsu Province of China for Domestic Animal Germplasm Resources and Genetic Improvement, Yangzhou 225000, China*

[3] *International Livestock Research Institute (ILRI), P.O. Box 5689, Addis Ababa, Ethiopia*

[4] *Dankook University, 119, Dandae-ro, Cheonan 31116, Republic of Korea*

[5] *Department of Animal Production, Jordan University of Science and Technology (JUST), P.O. Box 3030, 22110 Irbid, Jordan*

[6] *Meat Processing Key Laboratory of Sichuan Province, College of Food and Biological Engineering, Chengdu University, Chengdu 610106, China*

Highlights

- Sulforaphane (SFN) has been identified to possess antioxidant and anti-inflammatory effects in the liver.
- SFN has been found to achieve the purpose of anti-inflammatory and antioxidant stress by facilitating the interaction between NR1D1 and NRF2.
- SFN has been discovered to induce lysine β-hydroxybutyrylation, an epigenetic modification in the liver, which is also involved in the regulation of oxidative stress.

Abstract

Sulforaphane (SFN) is a naturally occurring isothiocyanate found in cruciferous vegetables known for its anti-inflammatory and antioxidant effects in the body. However, whether its dietary addition impacts porcine liver health remains unclear, and if it does, the mechanisms are unknown. In this study, supplementing the diet of growing pigs with 1 g kg^{-1} SFN was found to improve growth performance and hepatocellular proliferation. Further analyses revealed that SFN reduced hepatic and serum malondialdehyde levels, while increasing glutathione peroxidase (GSH-PX) activity in the liver. Transcriptomic and proteomic studies demonstrated that SFN down-regulated multiple pathways, including oxidative phosphorylation, inflammatory responses, IL-6-JAK-STAT3 signaling, and TNFα signaling *via* NFκB. Meanwhile, it upregulated NRF2/GPX4/HO-1 expression and reduced IL-6 and TNFα expression. Mechanistic studies identified potential NR1D1 and NRF2 binding elements in the promoters of the *GPX4* and *HO-1* genes in the liver. Furthermore, metabolomic profiling revealed a decline in serum β-hydroxybutyrate levels after the administration of SFN, while further analysis confirmed that SFN enhanced a type of epigenetic modification in the liver, lysine β-hydroxybutyrylation (Kbhb). These results highlight the protective roles of SFN against liver inflammation and oxidative damage, and a novel mechanism involving NRF2 and NR1D1 synergy is proposed, although the promotion of hepatic Kbhb by SFN still requires further exploration.

Keywords: sulforaphane, anti-oxidative, NR1D1, lysine β-hydroxybutyrylation

1. Introduction

In intensive pig farming, a high-density breeding method is adopted to save feeding space (Hao *et al*. 2021). However, this approach can result in limited activity space, elevated environmental temperatures, and increased likelihood for bacterial infections, among other challenges. These factors can induce free radical production in pigs, disrupt their bodily balance, and cause oxidative stress and damage

Received 6 August 2024; Received in revised form 15 November 2024; Accepted 25 December 2024; Available online 17 February 2025
Yiting Wang, E-mail: ytwang1631@outlook.com; #Correspondence Demin Cai, E-mail: demincai@yzu.edu.cn; Zhaojian Li, E-mail: 007919@yzu.edu.cn

doi: 10.1016/j.jia.2025.02.019

(Wolter *et al*. 2003). Oxidative stress exerts detrimental effects on pigs at all stages of development. For instance, during late pregnancy and lactation, sows subjected to oxidative stress may suffer from impaired fetal development and reduced milk yield (Li *et al*. 2022). Pigs during the weaning and fattening phases may exhibit reduced feed intake, as well as compromised feed conversion efficiency and immune responses due to oxidative stress, potentially affecting the quality of related animal products (Zhang 2023). Consequently, prolonged and severe oxidative stress can negatively impact the economics of the pig farming industry. In this regard, nutritional strategies, including dietary supplements that may mitigate oxidative stress and improve health, have become essential for pig management.

Understanding the complex interplay between oxidative stress and inflammation is crucial for developing the means to control their adverse effects and reduce damage in pigs. These processes are intricately linked in numerous physiological and pathological contexts (Al Olayan *et al.* 2020). Oxidative stress refers to dysregulation between the production of reactive oxygen species (ROS) and the body's antioxidant defense mechanisms, culminating in cellular dysfunction and damage (van der Pol *et al.* 2019). Meanwhile, inflammation is the immune system's response to detrimental stimuli, such as tissue injury or pathogen invasion, and is characterized by the activation of immune cells and the release of inflammatory mediators (Abdulkhaleq *et al.* 2018). Oxidative stress triggers pro-inflammatory signaling, which promotes inflammation through the generation of cytokines and chemokines (Forrester *et al.* 2018). In turn, inflammation can exacerbate oxidative stress by fostering ROS production and disrupting antioxidant defense mechanisms. The liver plays a crucial role in maintaining the redox balance, by neutralizing free radicals through the secretion of antioxidant enzymes, thereby protecting the body from oxidative damage (Blas-García and Apostolova 2023). However, a prolonged state of oxidative stress can break this balance, resulting in severe liver damage (Allameh *et al.* 2023). This damage further impacts immune and metabolic functions throughout the body, triggering systemic health issues. Therefore, mitigating oxidative stress and inflammatory responses in the liver is of paramount importance.

Over the past few decades, broccoli has gained popularity as a dietary component due to its health-promoting properties, ranging from inflammatory modulation to enhancing intestinal well-being (Holman *et al.* 2023) and preventing cancer (Nestle 1998). As a cruciferous plant, broccoli contains numerous isothiocyanates, which originate from glucosinolates by a unique substrate-enzyme system known as the glucosinolate-myrosinase system. Among these isothiocyanates, sulforaphane (SFN) stands out for its significant health benefits particularly its antioxidant activity (Dinkova-Kostova and Kostov 2012). In the gut of mammals, broccoli intake prompts the conversion of glucoraphanin to SFN, which is then converted to dithiocarbamates through the mercapturic acid pathway, and ultimately excreted from the body (Yagishita *et al.* 2019). Current research indicates that the regulatory effects of SFN on oxidative stress and inflammation are primarily mediated through the modulation of nuclear factor erythroid 2-related factor 2 (NRF2) (Wu *et al.* 2022; Etemadi *et al.* 2023; Zhang *et al.* 2023). The impact of SFN on NRF2 further regulates pathways or factors associated with oxidative stress and inflammation, thereby enhancing overall health (Dong *et al.* 2016; Yi *et al.* 2018; Saleh *et al.* 2019; Wang *et al.* 2022; Zaghlool *et al.* 2023). However, whether SFN achieves its anti-inflammatory and antioxidant effects through other pathways remains unknown, as are the relevant mechanisms if it does.

Nuclear receptors are a class of transcription factors capable of binding small molecule ligands to regulate the expression of target genes in many pathways. Previous studies demonstrated that oxidative stress and inflammation are highly susceptible to regulation by transcription factors (He *et al.* 2020). Specifically, REV-ERBα, also known as NR1D1, is a nuclear receptor responsible for regulating the circadian clock. Emerging evidence suggests NR1D1 also plays a regulatory role in immunity (Amir *et al.* 2018; Chang *et al.* 2019), inflammation (Migita *et al.* 2004), bile acid synthesis (Duez *et al.* 2008), and lipid and glucose metabolism (Kumar *et al.* 2010). Therefore, this study used pigs to explore the antioxidant and anti-inflammatory properties of SFN in the liver and to ascertain the role of the nuclear receptor NR1D1 in regulating these beneficial effects. In addition, given that oxidative stress and inflammation affect the state of epigenetic modifications (Kowluru 2023), and orphan nuclear receptors can alter epigenetic modifications through interactions with DNA, histones, or other transcription factors (Tian *et al.* 2015), we also focused on hepatic epigenetic variations following SFN treatment.

2. Materials and methods

2.1. Animals and sampling

A total of 12 Duroc×(Landrace×Yorkshire) barrows at 50 d of age, with body weight (BW, 15±0.5 kg), were housed in enclosed pens that complied with animal welfare standards, including an appropriate stocking density, suitable lighting and temperature conditions, and a clean environment. They were randomly divided into two groups: the control group received a basal diet, and the SFN group was provided with a basal diet supplemented with SFN (1 g kg^{-1}). The basal diet was formulated to meet or exceed the nutrient requirements of weaned piglets as specified by the Chinese National Feeding Standard of Swine (Ministry of Agriculture and Rural Affairs of China, 2020). The specific diet formulation is presented in Table 1.

Pigs had free access to water and feed during the 60-d feeding trial. BW was monitored every 3–5 d and after a 12 h fast at the end of the trial. The pigs were euthanized by injection of sodium pentobarbital and immediately slaughtered. Blood was collected by jugular vein puncture and centrifuged at 3,000 r min^{-1} for 15 min to collect serum. The liver was collected and preserved at –80°C.

2.2. Blood analysis

Hematological analysis was performed within 2 h of sampling. The indices measured included white blood cell (WBC) count, neutrophil (Neu) count, lymphocyte (LYM)count, and

Table 1 Feed composition and ratios

Item	Content
Ingredients	
Corn (%)	68.00
Soybean meal (%)	16.00
DDGS(%)	3.00
Cottonseed meal (%)	2.00
Peanut meal (%)	3.00
Corn germ meal (%)	2.00
Calcium hydrogen phosphate (%)	1.30
Limestone powder (%)	0.35
Salt (%)	0.35
Pre-mixed feed (%)[1)]	4.00
Total (%)	100.00
Nutritional level	
Digestible energy (MJ kg^{-1})[2)]	13.95
Crude protein (%)[3)]	15.56
Crude fiber (%)[3)]	5.15
Ash content (%)[3)]	7.01
Calcium (%)[3)]	0.80
Phosphorus (%)[3)]	0.57
Lysine (%)[3)]	0.98
Methionine (%)[3)]	0.32

[1)] Per kilogram of premix content: Calcium 3.77 g, phosphorus 1.02 g, magnesium 3.10 g, potassium 1.50 g, sodium 0.37 g, chlorine 0.11 g, sulfur 84.00 g, iron 120,493 mg, copper 29,791 mg, cobalt 52.62 mg, magnesium 24,076 mg, zinc 134 mg, iodine 238 mg, selenium 476 mg, retinol 5,952,000 IU, choline iron complex 595,200 iu, α-tocopherol 101,190 mg, thiamine 2,381 mg, riboflavin 5,952 mg, pyridoxine 3,750 mg, vitamin B1 224 mg, pantothenic acid 11,914 mg, niacin 23,810 mg, biotin 2,238 mg.
[2)] Calculated values.
[3)] Values determined by analysis; each value is based on triplicate determination.

platelet (PLT) count. Serum metabolites, including aspartate aminotransferase (AST), alanine transaminase (ALT), alkaline phosphatase (ALP), total protein (TP), albumin (ALB), cholesterol (CHO), triglyceride (TG) and total bile acids (TBA), were determined using an automatic biochemical analyzer (ALOVSION LIC200, Suzhou, China) according to the manufacturer's instructions.

2.3. Hemotoxylin and Eosin (H&E) staining

Liver tissues were fixed in 4% paraformaldehyde for 12 h, dehydrated using ethanol and xylene, and embedded in paraffin. Tissues were cut into 4 μm slices and sections sequentially immersed in xylene, followed by re-hydration using 100%, 95%, and 70% ethanol. Then sections were incubated with hematoxylin at room temperature for 8 min and washed with water. After differentiation with 1% acidic ethanol, sections were stained with eosin for 30 s and rinsed for another 5 min. Images were obtained using a light microscope (Leica, DMi8 S, Germany). The average number of hepatocytes was obtained by counting 10 different views per section, and the cell cross-sectional area was calculated using ImageJ software (Fiji, Maryland, USA, version 1.0).

2.4. Detection of hepatic DNA and RNA contents

A well-established method for monitoring cell cycle and proliferation is measuring DNA content (Clark*et al.* 1989; Ligasová and Koberna 2021). Likewise, the RNA content in cells, which is also a potential indicator of cell proliferation and division (Hiraki 1994), was determined. Since DNA content is positively linked to cell proliferation and the cellular RNA content remains stable, the status of cell proliferation in the liver could be reflected by the DNA content and the ratio of DNA content to RNA. Hepatic DNA and RNA were extracted using the TRIzol sequential extraction method (ThermoFisher Scientific Inc. 2016). Nucleic acids from 100 mg of liver tissue were extracted with ethanol and chloroform-methanol. DNA and RNA were separated based on their different hydrolytic characteristics. Each DNA and RNA sample extracted from tissue was dissolved in 50 μL of solvent, while ensuring equal volumes of the upper aqueous phase and the lower organic phase during extraction. The final concentration was determined using a NanoReady F-3100 spectrophotometer (Life Real, Hangzhou, China).

2.5. GSH-PX, T-SOD, MDA, CAT, T-AOC, β-hydroxybutyrate (BHB) determination

The MDA concentration and enzymatic activities of GSH-PX, T-SOD, CAT, and T-AOC in the liver and serum were detected using commercial kits (Nanjing Jiancheng Bioengineering Institute, Nanjing, China). First, the liver tissue was homogenized with PBS at a ratio of 1:9 (g:mL^{-1}) and the protein concentration was determined with a BCA Protein Assay Kit (CWBiotech, Beijing, China). Liver homogenate and serum were used to determine the anti-oxidative enzyme activities and MDA content, according to the manufacturer's instructions.

The BHB concentration was measured using a commercial assay kit (Promega, USA). Liver tissue was processed, and the resulting tissue homogenate was used to determine the BHB content according to the manufacturer's instructions.

2.6. Western blot assay

The hepatic proteins were obtained by homogenizing samples with radio-immunoprecipitation assay (RIPA) lysis buffer containing phenylmethanesulfonyl fluoride (PMSF), followed by centrifugation at 12,000×g for 10 min at 4°C. The protein concentration was determined, and 30 μg of protein from each sample was loaded on 8–12% sodium dodecyl sulfate (SDS)-polyacrylamide gels and transferred onto polyvinylidene difluoride (PVDF) membranes (Millipore, MA, USA). The membranes were blocked with 5% skimmed milk for 1 h before overnight incubation with the primary antibody at 4°C, followed by 1 h incubation with horseradish peroxidase (HRP)-conjugated secondary antibodies at room temperature. Finally, the membranes were visualized using an automatic chemiluminescence imaging analysis system (Tanon, Shanghai, China) and a Chemiluminescent Detection Kit (Vazyme, Nanjing, China). Western blot bands were quantified using ImageJ software. The antibodies used are shown in Table 2.

2.7. RNA-seq analysis

Hepatic RNA was extracted using TRIzol (Invitrogen, CA, USA), and its concentration and quality were assessed using an Agilent 2100 bioanalyzer (Agilent Technologies, Palo Alto,

Table 2 Antibodies utilized in Western blot analysis

Antibody	Brand	Catalogue no.	Dilution rate
β-actin	Proteintech	20536-1-AP	1:10,000
CDK4	Proteintech	11026-1-AP	1:1,000
PCNA	Proteintech	10205-2-AP	1:1,000
GPX4	Proteintech	67763-1-IG	1:1,000
HO-1	Proteintech	10701-1-AP	1:1,000
TNF-α	Proteintech	60291-1-IG	1:1,000
IL-6	Proteintech	21865-1-AP	1:1,000
NR1D1	Cell signaling technology	13418T	1:1,000
NRF2	Proteintech	16396-1-AP	1:1,000
H3K9bhb	PTM Biolabs	PTM1250	1:1,000
H3K9ac	Immuno way	Ym3268	1:1,000
H3K18bhb	PTM Biolabs	PTM-306RM	1:1000
H3K18ac	Epigentek	A-4024-100	1:1000
H3	Abcam	ab1791	1:1000

CA, USA). Oligo(dT) bead enriched eukaryotic mRNA was fragmented into short fragments and reverse transcribed into cDNA using the NEBNext Ultra RNA Library Prep Kit for Illumina (NEB #7530, New England Biolabs, Ipswich, MA, USA). The purified double-stranded cDNA fragments were end-repaired and ligated to Illumina sequencing adapters. The ligation reaction product was purified with AMPure XP Beads (1.0X) and amplified by polymerase chain reaction (PCR). The resulting cDNA library was sequenced on an Illumina Novaseq 6000 platform by Gene Denovo Biotechnology Co. (Guangzhou, China). The threshold of differentially expressed genes (DEGs) was set as $|\log_2(\text{fold change})|>1$ and adjusted $P<0.05$.

2.8. Kyoto Encyclopedia of Genes and Genomes (KEGG) and Gene Ontology analysis (GO)

Gene Set Enrichment Analysis (GSEA 4.1.0) software was used to identify the HALLMARK and KEGG pathways enriched in DEGs. Furthermore, the statistically enriched biological processes or pathways of SFNs were ranked and classified using the David database (Sherman *et al.* 2022) (https://david.ncifcrf.gov) for GO pathways. An online platform (http://www.bioinformatics.com.cn) was used for data analysis and visualizing the HALLMARK and KEGG pathway plots. The volcano plot was visualized using GraphPad Prism (version 9.5).

2.9. LC-MS metabolic analysis

The metabolome of serum was analyzed using a Waters UPLC I-Class Plus System (Waters, USA) in tandem with a Q exactive high-resolution mass spectrometer (ThermoFisher Scientific, USA) for metabolite separation and detection. The downstream data of the mass spectrometry were imported into Compound Discoverer 3.3 (ThermoFisher Scientific) software and the mass spectrometry data were analyzed in conjunction with the BMDB (BGI Metabolome Database), mzCloud and Chem Spider online databases. A data matrix containing information such as metabolite peak areas and identification results was obtained.

The data were then imported into the Metaboanalyst (https://www.metaboanalyst.ca/) online website for preprocessing, including peak realignment, baseline correction, sample quality check, and peak deconvolution. Multivariate statistics, such as principal component analysis (PCA) and orthogonal partial least squares-discriminant analysis (OPLS-DA), were performed using SIMCA software (version 14.1). Candidate variables with variable importance in the projection (VIP)>1.0 and P-value<0.05 were considered statistically significant. Enrichment analysis and pathway enrichment analysis were also conducted on the Metaboanalyst platform website.

2.10. ChIP-qPCR

Liver tissues snap-frozen in liquid nitrogen were ground into powder. The powdered tissues were resuspended in a fixation buffer of 50 mmol L^{-1} HEPES-KOH, 100 mmol L^{-1} NaCl, 1 mmol L^{-1} EDTA, and 0.5 mol L^{-1} EGTA before being crosslinked with 1% formaldehyde for 5 min. The crosslinking reaction was terminated by the addition of cold glycine for 6 min. The collected precipitates were resuspended using lysis solution (50 mmol L^{-1} HEPES pH=8.0, 140 mmol L^{-1} NaCl, 1 mmol L^{-1} EDTA, 10% glycerol, 0.5% NP40, 0.25% Triton X). They were washed with a buffer composed of 10 mmol L^{-1} Tris-HCl pH8.0, 1 mmol L^{-1} EDTA, 0.5 mmol L^{-1} EGTA, and 200 mmol L^{-1} NaCl, followed by resuspension of the precipitates in shear buffer (0.1% SDS, 1 mmol L^{-1} EDTA pH=8.0, 10 mmol L^{-1} Tris-HCl pH8.0) and sonicated using a Covaris M220 instrument. Chromatin fragments were precipitated by gene-specific antibodies and protein G-coupled magnetic beads and then treated with RNase A and proteinase K. ChIP-ed-DNA obtained by purification was used for qPCR analysis. The primers used for qPCR are listed in Appendix A, and the antibodies used for ChIP are shown in Table 3.

2.11. ChIP-re-ChIP

The materials and procedures described in the ChIP-qPCR were used for the ChIP-re-ChIP analysis. Liver tissues were frozen, powdered, and fixed in a buffer. After formaldehyde crosslinking and glycine treatment, samples were lysed, washed, and sonicated. Chromatin was immunoprecipitated with gene-specific antibodies, and fragments were treated with RNase A and proteinase K. The ChIP-ed-DNA obtained was used as samples for a second round with an antibody. The DNA acquired from this second operation was used for qPCR analysis. The primers used for qPCR are listed in Appendix A, and the antibodies used for ChIP are shown in Table 3.

2.12. Statistical analysis

Statistical analysis was performed with GraphPad Prism 9.5.1

Table 3 Antibodies utilized in ChIP

Antibody	Brand	Catalogue no.	Dilution rate
NR1D1	Cell Signaling Technology	13418T	1:1,000
NRF2	Proteintech	16396-1-AP	1:1,000
SRC-1	Cell Signaling Technology	2191T	1:1,000
SRC-3	Cell Signaling Technology	2126T	1:1,000
NCOR1	Bioworld	BS78821	1:1,000
NCOR2	Bioworld	BS71201	1:1,000

software by Student's *t*-test to compare the means, and data are shown as mean±SEM. Differences were considered significant when $P<0.05$. All figures were generated using GraphPad Prism 9.5.1 software.

3. Results

3.1. SFN supplementation promoted growth performance and hepatocyte proliferation

Dietary supplementation with SFN significantly increased body weight in the last two weeks of the trial ($P<0.05$), with no difference observed in feed intake (Fig. 1-A and B). Regarding the potential hepatic effects of SFN, first, a histological examination of the liver was performed to identify any pathological alterations (Fig. 1-C). The hepatic triad structures in the portal areas of the SFN and control groups were found to be morphologically intact. The interlobular veins exhibited typical large diameters with thin and irregular walls, whereas the interlobular arterioles displayed small diameters, narrowed lumens, and thickened walls. Second, a significant increase in the number of hepatocytes ($P<0.05$, Fig. 1-D) and reduction in cell size ($P<0.05$, Fig. 1-E and F) were observed in the SFN group compared to the control. Dietary SFN supplementation also significantly increased the hepatic DNA content ($P<0.05$, Fig. 1-G) with an influence on RNA content (Fig. 1-H), resulting in a higher ratio of DNA to RNA ($P<0.05$, Fig. 1-I).

3.2. SFN modulated the expression of genes in pathways involved in oxidative stress and inflammation in the liver

Serum levels of TP and ALB, established biomarkers of liver inflammation, remained unchanged following SFN administration (Fig. 2-A and B). The assessment of hepatic injury markers revealed no significant differences in serum ALT and ALP levels between the groups (Fig. 2-C and E), while the SFN group displayed a slightly reduced serum AST level ($P<0.05$, Fig. 2-D). Furthermore, hepatic lipid metabolites, including TG, CHO, and TBA, were significantly reduced in the SFN group ($P<0.05$, Fig. 2-F–H). The RNA-seq data was consistent with the above results, while pathways closely associated with cytogenesis were up-regulated by SFN treatment (Fig. 3-E). In contrast, apoptotic pathways were down-regulated (Fig. 3-I) after SFN administration. A heatmap listing the altered genes involved in the apoptosis signaling pathway was generated (Fig. 3-N). The SFN group exhibited significant increases in the expression of CDK4 and PCNA, well-established markers for cell proliferation, as determined by Western blot analysis ($P<0.05$, Fig. 5-A–C). These findings indicate that SFN treatment elevates liver cytopoiesis and reduces hepatocyte apoptosis..

The LC-MS analysis revealed dynamic changes in serum metabolites in pigs fed SFN. A total of 727 metabolites were detected, primarily belonging to categories of organic acids and derivatives (29.14%), lipids and lipid-like molecules (21.7%), and organoheterocyclic compounds (17.33%) (Fig. 4-A). The PCA score plots and OPLS-DA analysis demonstrated a clear separation of the serum metabolic profiles between the SFN group and the control (Fig. 4-B and C).

Specifically, metabolites with VIP value>1.0 and $P<0.05$ were identified as potential metabolic markers (Fig. 4-D), and a heatmap of peak intensity was produced (Fig. 4-E). Some sulfate-related metabolites, such as guaiacol sulfate and

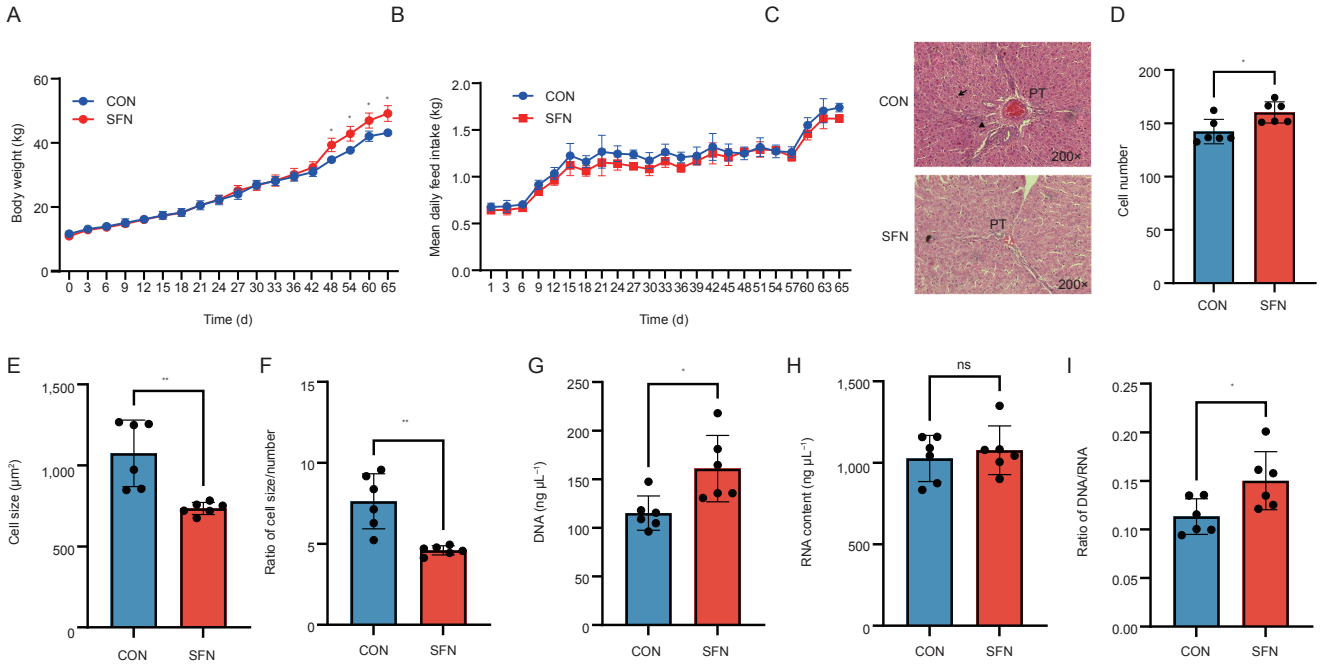

Fig. 1 Effects of dietary sulforaphane (SFN) on body weight, feed intake, hepatic histology, hepatocyte morphology, and hepatic nucleic acid content. A, body weight gain curve. CON, the control. B, mean daily feed intake curve of pigs. C, H&E-stained sections of the liver at 200x under the light microscope. PT means portal area. Arrows point to Kupffer cells, and triangles to blood hepatic sinusoid epithelial cells. D–F, relative cell number (D), cell size (E), and ratio of cell size to cell number (F). G–I, contents of DNA and RNA, and the ratio of DNA to RNA. *, $P<0.05$; **, $P<0.01$.

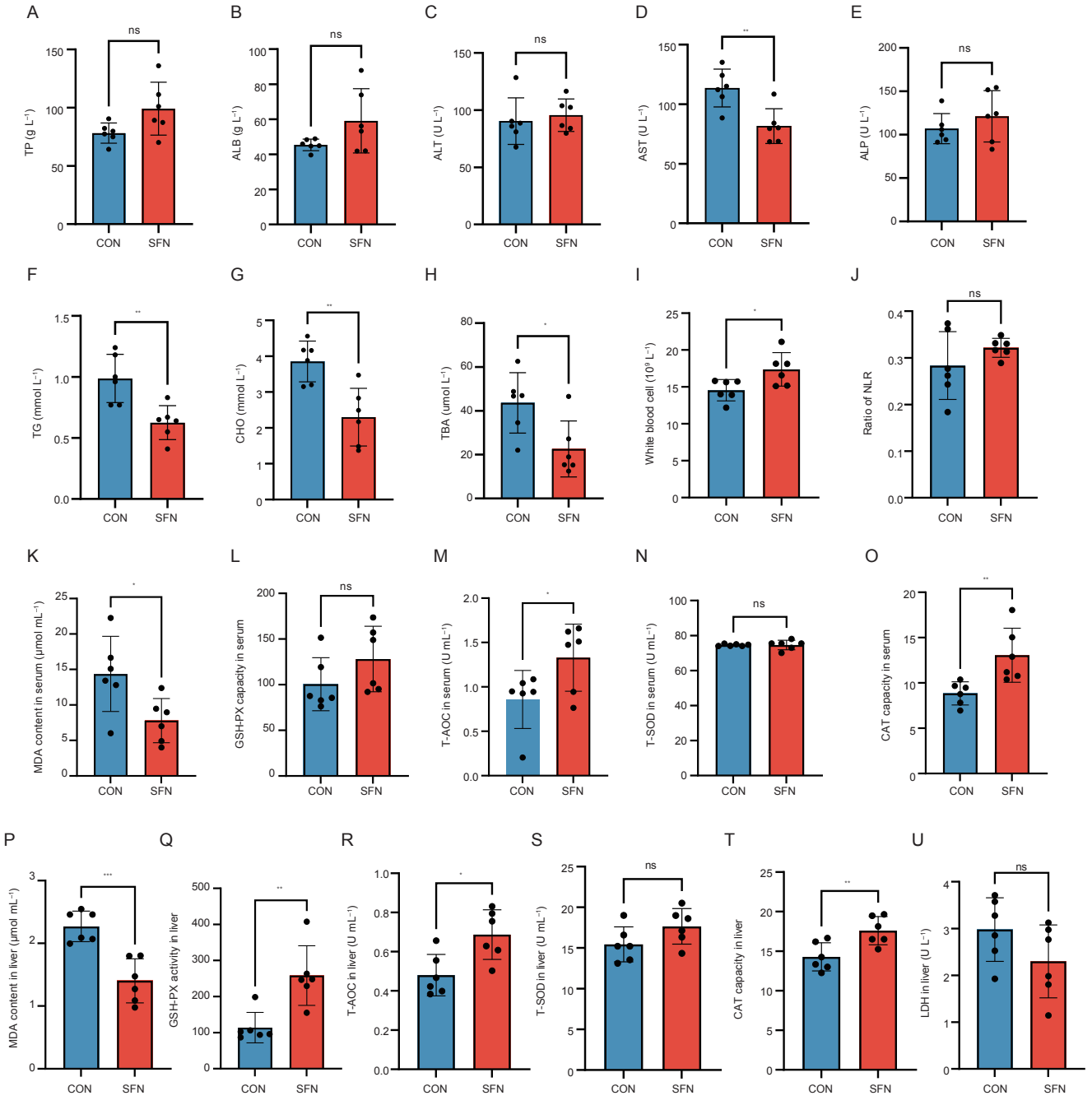

Fig. 2 Effects of dietary sulforaphane (SFN) on serum liver-related biochemical indices, hepatic lipid metabolites, oxidative stress biomarkers, antioxidant enzyme activities, and peripheral blood cell counts. A and B, biochemical indicators reflecting the level of liver inflammation like total protein (TP) and albumin (ALB). CON, the control. C–E, biochemical test of liver function with alanine transaminase (ALT), aspartate aminotransferase (AST), and alkaline phosphatase (ALP). F–H, biochemical indicators reflecting the liver lipid level. TG, triglyceride; CHO, cholesterol; TBA, total bile acids. I and J, two indicators of inflammation: the number of white blood cells and the ratio of neutrophils to lymphocytes (NLR) in the blood components. K–T, indicators of oxidative stress in the serum and liver: malondialdehyde (MDA), glutathione peroxidase (GSH-PX), total antioxidant capacity (T-AOC), total superoxide dismutase (T-SOD) and catalase (CAT). U, lactate dehydrogenase (LDH) in the liver. *, $P<0.05$; **, $P<0.01$.

tauroursodeoxycholic acid, were increased in the SFN group.

Metaboanalyst (https://www.metaboanalyst.ca) was used to classify the metabolic markers by the Small Molecule Pathway Database (SMPD) enrichment analysis and KEGG pathway analysis, which yielded seven metabolic processes (Fig. 4-F, $P<0.05$) and 10 pathways (Fig. 4-G, $P<0.05$). These SFN-enriched metabolic processes and pathways included pyrimidine metabolism, β-alanine metabolism, phenylalanine metabolism and histidine metabolism.

3.3. SFN supplementation mitigates serum inflammatory responses and oxidative stress in the liver

Transcriptome analysis was performed to determine the key transcriptional pathways influenced by dietary SFN. A total

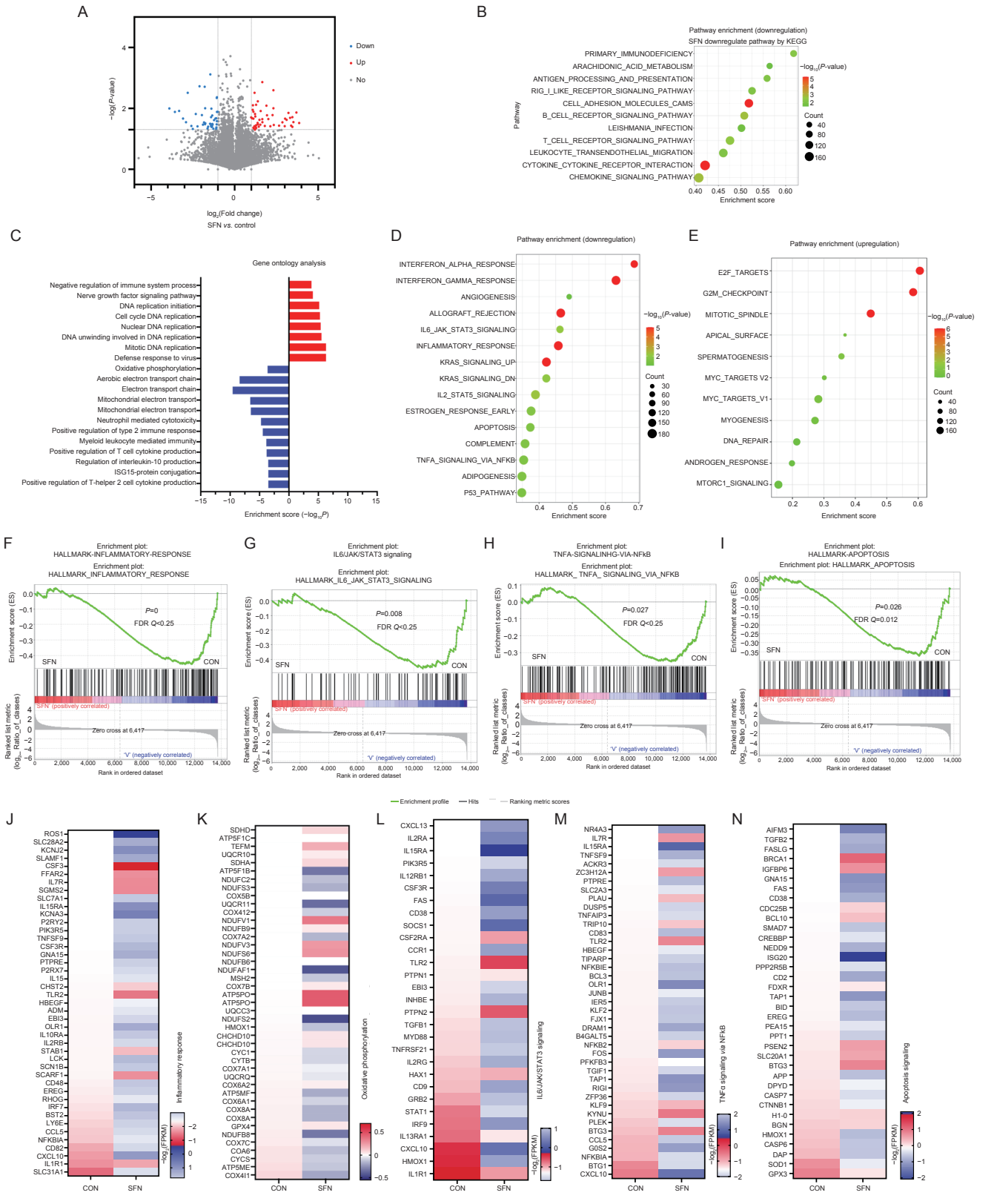

Fig. 3 RNA-seq analysis of transcriptome following dietary sulforaphane (SFN) supplementation. A, volcano plot visualizing the differential gene expression profiles between the SFN and control group by transcriptome analysis $|\log_2(\text{fold change})|>1$ and adjusted $P<0.05$. CON, the control. B, expression of genes involved in the inflammatory-related and immune-related pathways were among the most enriched pathways analyzed by KEGG. C, expression of genes involved in the oxidative phosphorylation pathway were among the most enriched pathways analyzed by GO analysis. D, expression of genes involved in the inflammatory-related and immune-related pathways were the most enriched pathways analyzed by HALLMARK. E, the pathways related to cytopoiesis were enriched after SFN treatment. F–H, enrichment plot from GSEA for the inflammatory response, IL6/JAK/STAT3, and TNF-α signal *via* NF-kB pathways. I, GSEA depicting the enrichment downregulated in apoptosis after SFN treatment. J–N, heatmaps of mRNA expression (RNA-seq, $\log_2$transformed) from the enriched pathways mentioned above.

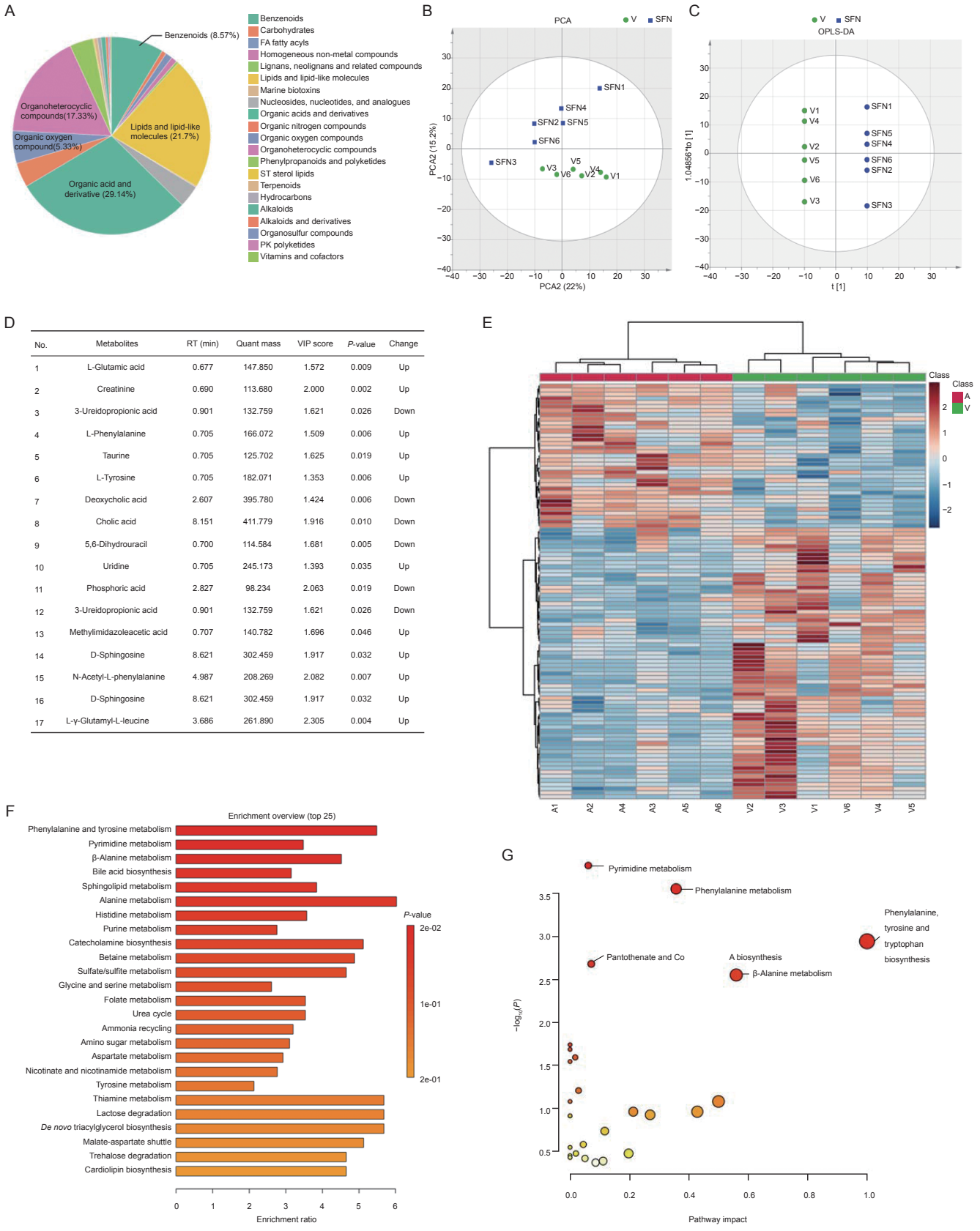

D

No.	Metabolites	RT (min)	Quant mass	VIP score	*P*-value	Change
1	L-Glutamic acid	0.677	147.850	1.572	0.009	Up
2	Creatinine	0.690	113.680	2.000	0.002	Up
3	3-Ureidopropionic acid	0.901	132.759	1.621	0.026	Down
4	L-Phenylalanine	0.705	166.072	1.509	0.006	Up
5	Taurine	0.705	125.702	1.625	0.019	Up
6	L-Tyrosine	0.705	182.071	1.353	0.006	Up
7	Deoxycholic acid	2.607	395.780	1.424	0.006	Down
8	Cholic acid	8.151	411.779	1.916	0.010	Down
9	5,6-Dihydrouracil	0.700	114.584	1.681	0.005	Down
10	Uridine	0.705	245.173	1.393	0.035	Up
11	Phosphoric acid	2.827	98.234	2.063	0.019	Down
12	3-Ureidopropionic acid	0.901	132.759	1.621	0.026	Down
13	Methylimidazoleacetic acid	0.707	140.782	1.696	0.046	Up
14	D-Sphingosine	8.621	302.459	1.917	0.032	Up
15	N-Acetyl-L-phenylalanine	4.987	208.269	2.082	0.007	Up
16	D-Sphingosine	8.621	302.459	1.917	0.032	Up
17	L-γ-Glutamyl-L-leucine	3.686	261.890	2.305	0.004	Up

Fig. 4 LC-MS-based metabolomics analysis of serum samples from sulforaphane (SFN)-supplemented pigs. A, categorical pie chart of metabolites measured by LC-MS. B, PCA score plots showing the metabolic patterns between the control and SFN groups. C, OPLS-DA plots for the SFN-treated and control groups. D, list of potential metabolic markers (VIP value>1.0 and P<0.05) characterized by LC-MS. E, heatmap of the differential metabolites enriched in the pathways above. Red represents the up-regulation of metabolites, while blue represents down-regulation. F, enrichment analysis of the critical metabolic markers (VIP value>1.0 and P<0.05). G, pathway analysis of the critical metabolic markers (VIP value>1.0 and P<0.05).

of 94 genes exhibited differential expression between the SFN and control groups, with 50 genes up-regulated and 44 genes down-regulated (Fig. 3-A). Notably, the Hallmark and KEGG pathway enrichment analyses indicated that the down-regulated genes were primarily associated with inflammatory and immune-related pathways (Fig. 3-B–D). The GSEA analysis indicated that the inflammatory response, IL6/JAK/STAT3 and TNF-α signal *via* NF-κB pathways were significantly downregulated by SFN (P<0.05, Fig. 3-F–H). In addition, GO analysis showed strongly down-regulated pathways involved in oxidative phosphorylation and immune responses in the SFN group (P<0.05, Fig. 3-C). A comprehensive examination of these three databases consistently highlighted the enrichment of pathways involved in the inflammatory response and immunity (Fig. 3-J–M), suggesting the crucial role of SFN in anti-inflammatory and anti-oxidative stress pathways.

To further validate the results of the transcriptome, oxidative stress indicators, including MDA, GSH-PX, T-AOC, CAT, and T-SOD, were detected. The serum and hepatic MDA concentrations in the SFN group were significantly lower compared to the control group (P<0.05, Fig. 2-K and P). Furthermore, the SFN group also displayed significantly higher hepatic activities of GSH-Px, T-AOC and CAT than the control group (P<0.05, Fig. 2-Q, R and T). No differences were found in the hepatic activities of T-SOD and LDH between groups (Fig. 2-S and U). In the serum, the activities of T-AOC and CAT were significantly improved by dietary SFN (P<0.05, Fig. 2-M and O), while the activities of GSH-Px and T-SOD displayed no changes after SFN administration (Fig. 2-L and N). Regarding the expression of antioxidant proteins, GPX4 and HO-1 displayed significantly higher expression in the SFN group than in the control group (P<0.05, Fig. 5-A, D and E).

In terms of blood composition data, the consumption of SFN led to an increase in white blood cell levels (P<0.05, Fig. 2-I). The neutrophil to lymphocyte ratio (NLR) has recently become an emerging indicator of the inflammatory response (Buonacera *et al.* 2022). No significant influence on NLR was observed after SFN administration (Fig. 2-J). The protein expression levels of TNF-α and IL-6, critical indicators of the inflammatory response, showed slight reductions in the SFN group (P<0.05, Fig. 5-A, F, and G).

3.4. SFN supplementation enhances the interaction between NR1D1 and NRF2 responses as well as the expression of anti-oxidative genes

The RNA-seq analysis of all nuclear receptors revealed that the SFN group displayed significantly enhanced expression of *NR1D1* mRNA (Appendix B-a), and NR1D1 protein expression in the SFN group was also higher than in the control group (P<0.05, Fig. 5-A and H). NRF2, a vital marker of the anti-oxidative pathway, was found to be significantly improved in protein expression after SFN administration (P<0.05, Fig. 5-A and I). To further investigate the relationship between NR1D1 and NRF2, we analyzed the ChIP-seq data derived from a previous report in mice (Adlanmerini *et al.* 2021). The classic DNA binding motif of NR1D1 is AGGTCA (Appendix B-b). Transcription factor (TF) motif analysis of NR1D1-peaked regions identified antioxidant response element (ARE) and NRF2 as the top-ranking motifs (Appendix B-c). Further analysis of the transcription factor motifs at the binding sites of NR1D1 demonstrated significant enrichment of motifs related to the NRF2 response elements within these regions, which were prominently ranked (Appendix B-c). These observations indicate that NR1D1 may be involved in the regulation of gene expression through interactions with *NRF2* response elements, consequently impacting the anti-inflammatory and antioxidant responses of the cell. GO analysis of the ChIP-seq peaks indicated that the oxidative stress pathway was one of the most significantly enriched biological processes (Appendix B-d). Further analysis of the ChIP-seq data in mice revealed that *Nr1d1* binds to the oxidative stress pathway. This binding was significantly enhanced when mice were fed a high-calorie diet (Appendix B-e and f). Similarly, the binding of *Nr1d1* to the archetypal antioxidant and inflammatory response genes, *Gpx4* and *Ho-1* (Feng *et al.* 2022), showed visible alterations following high-calorie diet treatment, further corroborating the regulatory role of NR1D1 in oxidative stress and inflammation (Fig. 6-C). Further analysis showed that the promoter regions of GPX4 and HO-1 contain motif sequences for NR1D1 and NRF2, and these motifs are in close proximity (Fig. 6-A and B). Similarly, the promoter region base sequences of *GPX4* and *HO-1* in pigs also displayed closely located motifs for NR1D1 and NRF2, respectively (Fig. 6-D–F). We further assessed these variations in the binding affinities of *GPX4* and *HO-1* to a panel of transcription factors, which indicated that SFN significantly enhanced the binding affinities of both *GPX4* and *HO-1* to NR1D1, NRF2, and nuclear receptor coactivator SRC-1 (P<0.05, Fig. 6-G–I). Another coactivator, SRC-3, also displayed a notable improvement in binding affinity to *HO-1* following treatment with SFN (P<0.05, Fig. 6-J). Regarding the binding to nuclear receptor corepressors, dietary SFN significantly reduced the binding affinity of NCOR2 to *GPX4* (P<0.05, Fig. 6-L) without influencing the binding affinity of NCOR1 to either of the genes (Fig. 6-K). The ChIP-re-ChIP assays further substantiated the significant association between these two transcription factors following SFN treatment (P<0.05, Fig. 6-M). Collectively, these results suggest that NR1D1 and NRF2 jointly carry out the regulation of oxidative stress and inflammation.

3.5. SFN supplementation modifies histones in the liver

The results from the assay kit showed a significant enrichment of BHB in the serum of pigs fed SFN (P<0.05, Fig. 7-A). BHB is typically produced during the oxidation of fatty acids and serves as an energy substrate during fasting or low carbohydrate availability (He *et al.* 2023). Recent research has also implicated BHB in epigenetic modifications, particularly through a novel post-translational protein modification known as lysine β-hydroxybutyrylation (Kbhb) (Huang *et al.* 2021). Hence, we further investigated the expression of epigenetic markers related to the BHB metabolic pathway. Our results showed that the expression of two key butyrylation proteins, H3K9bhb and

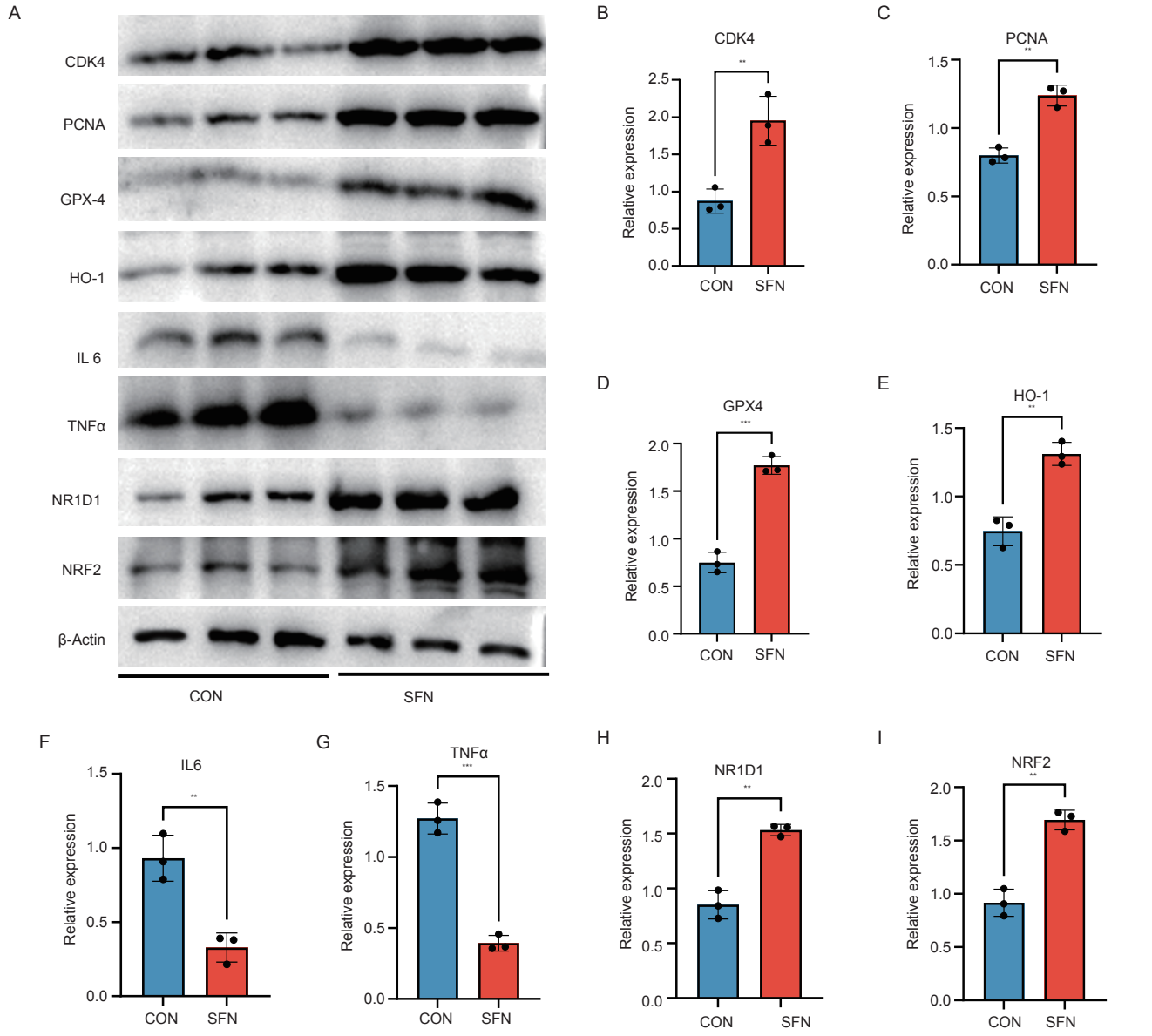

Fig. 5 Western blot analysis of hepatic protein expression in response to dietary sulforaphane (SFN). A, Western blot analysis of CDK4, PCNA, GPX4, HO-1, TNF-α, IL6, NRF2 and NR1D1 protein expression in the SFN group and the control (CON). β-actin was used as the loading control. B, relative protein expression of CDK4 was normalized to β-actin. C, relative protein expression of PCNA was normalized to β-actin. D, relative protein expression of GPX4 was normalized to β-actin. E, relative protein expression of HO-1 was normalized to β-actin. F, relative protein expression of IL-6 was normalized to β-actin. G, relative protein expression of TNF-α was normalized to β-actin. H, relative protein expression of NR1D1 was normalized to β-actin. I, relative protein expression of NRF2 was normalized to β-actin. **, $P<0.01$; ***, $P<0.001$.

H3K18bhb, were elevated following SFN treatment. SFN also slightly increased the expression of acetylated protein H3K9ac with no influence on H3K18ac expression (Fig. 7-B). The ChIP-qPCR results for Kbhb-related markers were consistent with the protein expression data, with both indicating that significant increases in the binding of *GPX4* and *HO-1* to Kbhb-related proteins were observed following treatment with SFN ($P<0.05$, Fig. 7-C and E). Meanwhile, SFN enhanced the binding of *GPX4* and *HO-1* to acetylation-related protein H3K18ac, and the binding of *GPX4* to H3K9ac protein was also significantly improved by SFN ($P<0.05$, Fig. 7-D and F).

4. Discussion

SFN is a naturally occurring isothiocyanate with numerous biological functions, and it has been extensively studied for its antioxidant and anti-inflammatory properties. These characteristics suggest the potential application of SFN in modulating liver and metabolic health. In this study, we examined the impact of SFN on porcine liver and metabolism, which revealed that dietary SFN not only enhances growth performance and hepatocyte proliferation but also exhibits significant antioxidant and anti-inflammatory effects in the liver *via* the NRF2/HO-1/GPX4 pathway. Further examination indicated that the nuclear receptor NR1D1 and ligand-

activated transcription factors, such as SRC-1 and SRC-3, participate in the NRF2-mediated up-regulation of HO-1 and GPX4. This finding sheds new light on SFN's mechanism of action in liver protection and metabolic regulation. Concurrently, our metabolomic analysis showed that SFN increases serum BHB levels and enhances hepatic histone butylation, as evidenced by elevated expression of the H3K9bhb and H3K18bhb proteins, which likely contribute to the enhancement of hepatic antioxidant capacity by SFN by promoting the binding of *GPX4* and *HO-1* genes to butylation-related proteinss.

Extensive research has assessed the safety of SFN as a food additive. Most functional studies on SFN have highlighted its roles in anti-inflammation, antioxidant activity, and the regulation of metabolic processes within the organism (Socała *et al*. 2017; Chartoumpekis *et al*. 2019). SFN has been characterized as a natural activator of transcription factor NRF2 (Ford and Bionaz 2024), which plays a critical role in the response to oxidative stress and inflammation. Research on insulin resistance demonstrated that dietary supplementation with SFN improved body weight and liver function and inhibited hyperlipidemia in high-fat-diet-fed mice by activating the AMPK-NRF2-GPX4 pathway (Zhang *et al.* 2022). Another study found that the administration of SFN activated the KEAP1-NRF2 anti-oxidative pathway, suppressed the generation of pro-inflammatory cytokines (IL-1β and IL-6), and significantly ameliorated the pathological symptoms and systemic inflammation in mice suffering from psoriasis (Ma *et al.* 2023). Collectively, these findings suggest that the beneficial effects of SFN on the organism may be mediated through the modulation of NRF2, consistent with our current results.

NRF2 is crucial in the anti-inflammatory and antioxidant stress regulatory mechanisms triggered by SFN. NRF2 is bound to KEAP1, which keeps NRF2 in the cytoplasm and restricts its activity. When oxidative stress occurs, an increase in ROS causes NRF2 to dissociate from KEAP1, enabling it to move to the nucleus and activate AREs (Bellezza *et al.* 2018). This activation boosts the expression of antioxidant enzymes like SOD and GST (Tossetta and Marzioni 2022). The upregulation of these enzymes aids in clearing excess ROS, thereby maintaining the redox balance within the organism. In other words, NRF2 occupies a "central" position within the network of anti-inflammatory and antioxidant mechanisms (Chen and Maltagliati 2018; Sajadimajd and Khazaei 2018; Saha*et al.* 2020).

Emerging evidence indicates that nuclear receptors also participate in the regulation of antioxidant and anti-inflammatory responses (Hong *et al*. 2021). As mentioned above, NR1D1 possesses modulatory functions in oxidative stress and inflammation (Yang *et al*. 2014). This study revealed that SFN administration prominently enhanced the expression levels of NR1D1, and the expression trend was highly consistent with that of NRF2 (Fig. 5-A). Meanwhile, a ChIP-seq data analysis by Marine Adlanmerini *et al*. (2021) further elucidated the connections between NR1D1 and NRF2. Considering the potent role of NRF2 in the transcriptional regulatory network, our results further demonstrated their relationship within this model, which was validated in our current study of SFN-fed pigs. We also studied the relationships between GPX4 and HO-1 with transcriptional cofactors. The cofactors SRC-1 and SRC-3 are members of the nuclear receptor coactivator family that enhance the transcriptional activity of nuclear receptors (Dasgupta *et al.* 2014; Gilad *et al.* 2022). Conversely, the two nuclear receptor corepressors NCOR1 and NCOR2 prevent the coactivators from binding to nuclear receptors, thereby inhibiting the transcriptional activity of target genes (Gurevich *et al.* 2007; Perissi *et al.* 2010; Kong *et al.* 2020). Our findings revealed that dietary SFN enhanced the binding of *GPX4* and *HO-1* to SRC-1 and SRC-3 and suppressed the binding to NCOR1 and NCOR2, which further confirmed that the transcriptional coactivators involved in NR1D1 and SFN activate the Nrf2/HO-1/GPX4 cascade.

Intriguingly, we observed epigenetic changes following SFN treatment. Variations in the β-hydroxybutyric acid levels obtained through the metabolomic analysis suggest a novel epigenetic modification, Kbhb, which has been identified as a new type of histone modification derived from β-hydroxybutyric acid (Zhang *et al*. 2019). This modification involves the covalent attachment of β-hydroxybutyrate, the main ketone body component, to the lysine residues of histones. Internal BHB levels increase during periods of fasting or low-carbohydrate intake. In addition to serving as an energy source, it possesses various biological functions, including energy metabolism, oncogenesis, and DNA damage repair (Koronowski *et al.* 2021; Zhou *et al.* 2022). Studies have shown Kbhb to be associated with the pathogenesis of metabolic cardiovascular diseases, renal diseases, tumors, neuropsychiatric disorders, and metabolic diseases (Zhang *et al.* 2020; Puchalska and Crawford 2021), so it possesses distinct functions compared to histone acetylation and methylation. Our results indicated that SFN enhanced the hepatic Kbhb epigenetic modifications. Typically, Kbhb acts in conjunction with other types of modifications, such as acetylation. Although, there were no observed changes in acetylation-associated proteins at the protein level, dietary SFN increased the binding of *GPX4* and *HO-1* to these proteins. These findings hint at a complex regulatory network involving Kbhb and acetylation, warranting further research to clarify their exact regulatory functions.

This study offers new insights into the antioxidant and anti-inflammatory mechanisms of SFN. However, it has several limitations. First, pig growth performance assessment involves multiple aspects, including body weight, feed intake, and health status (Rao *et al*. 2023). Here, the data only covered body weight and feed consumption, which are the two aspects of growth performance. We plan to measure additional indicators in future studies to better understand the impact of SFN on pig growth. Furthermore, as no studies exist on SFN supplementation in pig diets, the dosages used here were based on experiments with other animals (Xu *et al.* 2023), with the final dose similarly calculated. Future studies will build on these results to determine the optimal SFN

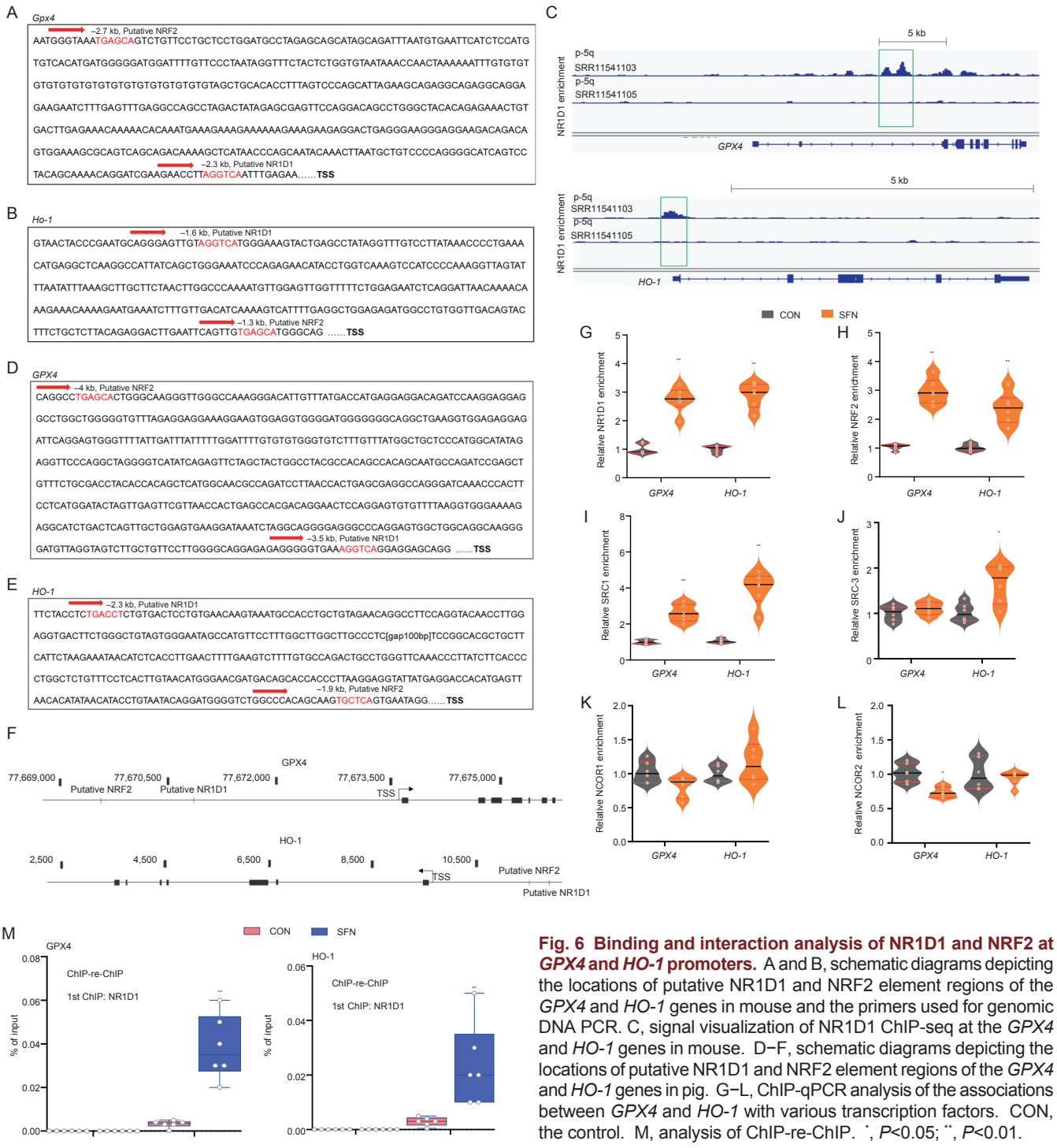

Fig. 6 Binding and interaction analysis of NR1D1 and NRF2 at *GPX4* and *HO-1* promoters. A and B, schematic diagrams depicting the locations of putative NR1D1 and NRF2 element regions of the *GPX4* and *HO-1* genes in mouse and the primers used for genomic DNA PCR. C, signal visualization of NR1D1 ChIP-seq at the *GPX4* and *HO-1* genes in mouse. D–F, schematic diagrams depicting the locations of putative NR1D1 and NRF2 element regions of the *GPX4* and *HO-1* genes in pig. G–L, ChIP-qPCR analysis of the associations between *GPX4* and *HO-1* with various transcription factors. CON, the control. M, analysis of ChIP-re-ChIP. *, $P<0.05$; **, $P<0.01$.

concentration for pig diets. In addition, since this experiment used a single *in vivo* concentration, it could not assess any dose-dependent effects of SFN in pigs. We are presently conducting further research into this phenomenon and plan to explore these effects at the cellular level. Lastly, due to the high production cost of SFN, collaboration with other industries to reduce the costs could promote its usage as a feed additive.

In this study, we reaffirmed the beneficial effects of SFN on the organism, especially the liver, and innovatively demonstrated that NR1D1 plays a role in SFN-mediated anti-inflammatory and antioxidant responses through the NRF2/GPX4/HO-1 pathway. We also observed the emergence of Kbhb following SFN treatment, and further analysis confirmed enhanced hepatic butyrylation modification. However, further research is needed to fully understand this novel epigenetic modification.

5. Conclusion

Our results demonstrate that dietary supplementation with SFN promotes growth performance and hepatocyte proliferation in growing pigs. Furthermore, SFN exhibits significant

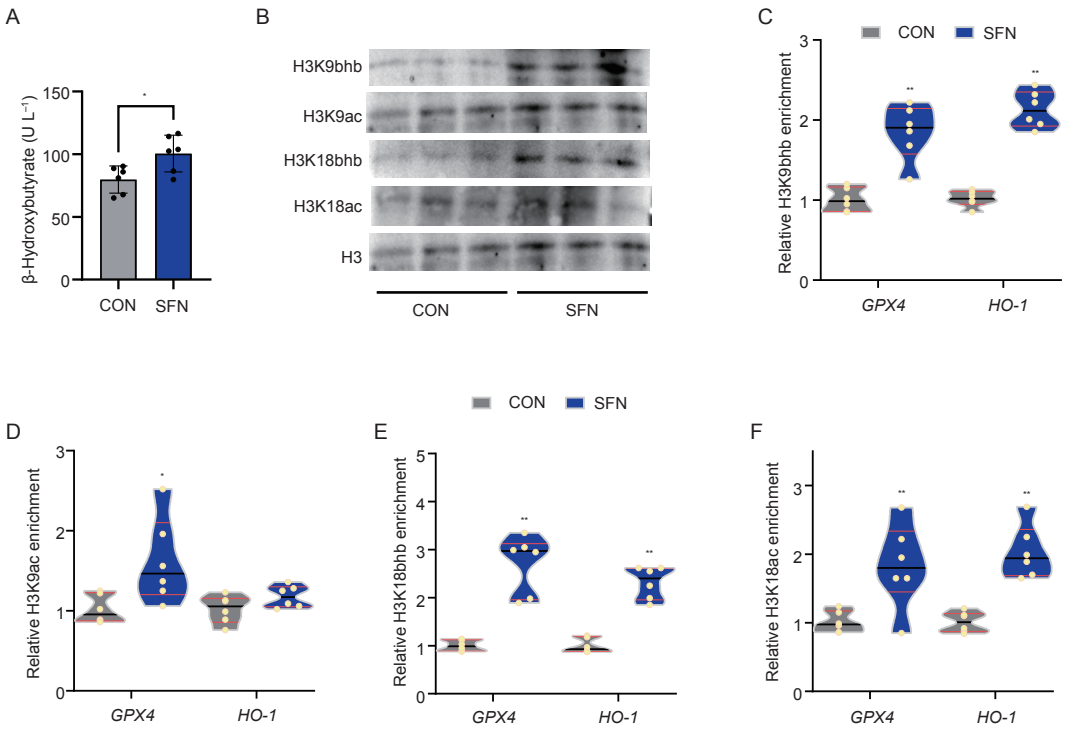

Fig. 7 Analysis of β-hydroxybutyrate (BHB)-associated epigenetic modifications on *GPX4* and *HO-1*. A, β-hydroxybutyrate levels. CON, the control. B, expression of proteins associated with Kbhb and acetylation. C–F, ChIP-qPCR analysis of the associations between *GPX4* and *HO-1* with various genes related to Kbhb and acetylation.

antioxidant and anti-inflammatory effects in the liver through the activation of the NRF2/HO-1/GPX4 cascade, involving NR1D1, transcriptional coactivators and histone butyrylation.

Acknowledgements

This work was funded by the National Key R&D Program of China (2023YFD1301200, 2021YFD1300205), the Jiangsu Provincial Double-Innovation Team Program, China (JSSCTD202147), the Natural Science Foundation of Jiangsu Province, China (BK20220582, BK20210812), the Priority Academic Program Development of Jiangsu Higher Education Institutions, China (PAPD), and the Open Project Program of the International Joint Research Laboratory in Universities of Jiangsu Province of China for Domestic Animal Germplasm Resources and Genetic Improvement.

Declaration of competing of interest

The authors declare that they have no conflict of interest.

Declaration of generative AI and AI-assisted technologies in the writing process

The authors declare that they did not use AI in the preparation and writing of this manuscript.

Ethical approval

The animal research proposal was approved by the Institutional Animal Care and Utilization Committee (IACUC) of the Animal Experimental Ethics Committee of Yangzhou University (permit number: SYXK(SU)IACUC2012-0029). The study was conducted in accordance with all local legislation and institutional requirements.

Appendies associated with this paper are available at https://doi.org/10.1016/j.jia.2025.02.019

References

Abdulkhaleq L A, Assi M A, Abdullah R, Zamri-Saad M, Taufiq-Yap Y H, Hezmee M N M. 2018. The crucial roles of inflammatory mediators in inflammation: A review. *Veterinary World*, **11**, 627–635.

Adlanmerini M, Nguyen H C, Krusen B M, Teng C W, Geisler C E, Peed L C, Carpenter B J, Hayes M R, Lazar M A. 2021. Hypothalamic REV-ERB nuclear receptors control diurnal food intake and leptin sensitivity in diet-induced obese mice. *Journal of Clinical Investigation*, **131**, e140424

Allameh A, Niayesh-Mehr R, Aliarab A, Sebastiani G, Pantopoulos K. 2023. Oxidative stress in liver pathophysiology and disease. *Antioxidants* (Basel), **12**, 1653.

Amir M, Chaudhari S, Wang R, Campbell S, Mosure S A, Chopp L B, Lu Q, Shang J, Pelletier O B, He Y, Doebelin C, Cameron M D, Kojetin D J, Kamenecka T M, Solt L A. 2018. REV-ERBα regulates TH17 cell development and autoimmunity. *Cell Reports*, **25**, 3733-3749.e8.

Bellezza I, Giambanco I, Minelli A, Donato R. 2018. Nrf2-Keap1 signaling in oxidative and reductive stress. *Biochimica et Biophysica Acta (BBA) — Molecular Cell Research*, **1865**, 721–733.

Blas-García A, Apostolova N. 2023. Novel therapeutic approaches to liver fibrosis based on targeting oxidative stress. *Antioxidants* (Basel), **12**, 1567

Buonacera A, Stancanelli B, Colaci, Malatino L. 2022. Neutrophil to lymphocyte ratio: An emerging marker of the relationships between the immune system and diseases. *International Journal of Molecular Sciences*, **23**, 3636

Chang C, Loo C S, Zhao X, Solt L A, Liang Y, Bapat S P, Cho H, Kamenecka T M, Leblanc M, Atkins A R, Yu R T, Downes M,

Burris T P, Evans R M, Zheng Y. 2019. The nuclear receptor REV-ERBalpha modulates Th17 cell-mediated autoimmune disease. *Proceedings of the National Academy of Sciences of the United States of America*, **116**, 18528–18536.
Chartoumpekis D V, Ziros P G, Chen J-G, Groopman J D, Kensler T W, Sykiotis G P. 2019. Broccoli sprout beverage is safe for thyroid hormonal and autoimmune status: Results of a 12-week randomized trial. *Food and Chemical Toxicology*, **126**, 1–6.
Chen Q M, Maltagliati A J. 2018. Nrf2 at the heart of oxidative stress and cardiac protection. *Physiological Genomics*, **50**, 77–97.
Clark G M, Dressler L G, Owens M A, Pounds G, Oldaker T, McGuire W L. 1989. Prediction of relapse or survival in patients with node-negative breast cancer by DNA flow cytometry. *The New England Journal of Medicine*, **320**, 627–633.
Dasgupta S, Lonard D M, O'Malley B W. 2014. Nuclear receptor coactivators: Master regulators of human health and disease. *Annual Review of Medicine*, **65**, 279–292.
Dinkova-Kostova A T, Kostov R V. 2012. Glucosinolates and isothiocyanates in health and disease. *Trends in Molecular Medicine*, **18**, 337–347.
Dong Z, Shang H, Chen Y Q, Pan L L, Bhatia M, Sun J. 2016. Sulforaphane protects pancreatic acinar cell injury by modulating Nrf2-mediated oxidative stress and NLRP3 Inflammatory pathway. *Oxidative Medicine and Cellular Longevity*, **2016**, 7864150.
Duez H, van der Veen J N, Duhem C, Pourcet B, Touvier T, Fontaine C, Derudas B, Baugé E, Havinga R, Bloks V W, Wolters H, van der Sluijs F H, Vennström B, Kuipers F, Staels B. 2008. Regulation of bile acid synthesis by the nuclear receptor Rev-erbalpha. *Gastroenterology*, **135**, 689–698.
Etemadi Y, Akakpo J Y, Ramachandran A, Jaeschke H. 2023. Nrf2 as a therapeutic target in acetaminophen hepatotoxicity: A case study with sulforaphane. *Journal of Biochemical and Molecular Toxicology*, **37**, e23505.
Feng J, Wang J, Wang Y, Huang X, Shao T, Deng X, Cao Y, Zhou M, Zhao C. 2022. Oxidative stress and lipid peroxidation: Prospective associations between ferroptosis and delayed wound healing in diabetic ulcers. *Frontiers in Cell and Developmental Biology*, **10**, 898657.
Ford H R, Bionaz M. 2024. The Experimental and in silico-based evaluation of nrf2 modulators, sulforaphane and brusatol, on the transcriptome of immortalized bovine mammary alveolar cells. *International Journal of Molecular Sciences*, **25**, 4264.
Forrester S J, Kikuchi D S, Hernandes M S, Xu Q, Griendling K K. 2018. Reactive oxygen species in metabolic and inflammatory signaling. *Circulation Research*, **122**, 877–902.
Gilad Y, Lonard D M, O'Malley B W. 2022. Steroid receptor coactivators — their role in immunity. *Frontiers in Immunology*, **13**, 1079011.
Gurevich I, Flores A M, Aneskievich B J. 2007. Corepressors of agonist-bound nuclear receptors. *Toxicology and Applied Pharmacology*, **223**, 288–298.
Hao Y, Xing M, Gu X. 2021. Research progress on oxidative stress and its nutritional regulation strategies in pigs. *Animals* (Basel), **11**, 1384
He F, Ru X, Wen T. 2020. NRF2, a transcription factor for stress response and beyond. *International Journal of Molecular Sciences*, **21**, 4777.
He Y, Cheng X, Zhou T, Li D, Peng J, Xu Y, Huang W. 2023. β-Hydroxybutyrate as an epigenetic modifier: Underlying mechanisms and implications. *Heliyon*, **9**, e21098.
Hiraki M 1994. Intracellular DNA RNA in the course of tumor cell growth. *The Kurume Medical Journal*, **41**, 1–13.
Holman J, Hurd M, Moses P L, Mawe G M, Zhang T, Ishaq S L, Li Y. 2023. Interplay of broccoli/broccoli sprout bioactives with gut microbiota in reducing inflammation in inflammatory bowel diseases. *The Journal of Nutritional Biochemistry*, **113**, 109238.
Hong T, Chen Y, Li X, Lu Y. 2021. The role and mechanism of oxidative stress and nuclear receptors in the development of NAFLD. *Oxidative Medicine and Cellular Longevity*, **2021**, 6889533.
Huang H, Zhang D, Weng Y, Delaney K, Tang Z, Yan C, Qi S, Peng C, Cole P A, Roeder R G, Zhao Y. 2021. The regulatory enzymes and protein substrates for the lysine β-hydroxybutyrylation pathway. *Science Advances*, **7**, eabe2771.
Kong Y, Zhou W, Sun Z. 2020. Nuclear receptor corepressors in intellectual disability and autism. *Molecular Psychiatry*, **25**, 2220–2236.
Koronowski K B, Greco C M, Huang H, Kim J K, Fribourgh J L, Crosby P, Mathur L, Ren X, Partch C L, Jang C, Qiao F, Zhao Y, Sassone-Corsi P 2021. Ketogenesis impact on liver metabolism revealed by proteomics of lysine β-hydroxybutyrylation. *Cell Reports*, **36**, 109487.
Kowluru R A. 2023. Cross Talks between oxidative stress, inflammation and epigenetics in diabetic retinopathy. *Cells*, **12**, 300.
Kumar N, Solt L A, Wang Y, Rogers P M, Bhattacharyya G, Kamenecka T M, Stayrook K R, Crumbley C, Floyd Z E, Gimble J M, Griffin P R, Burris T P. 2010. Regulation of adipogenesis by natural and synthetic REV-ERB ligands. *Endocrinology*, **151**, 3015–3025.
Li Q, Yang S, Chen F, Guan W, Zhang S. 2022. Nutritional strategies to alleviate oxidative stress in sows. *Animal Nutrition*, **9**, 60–73.
Ligasová A, Koberna K. 2021. DNA dyes-highly sensitive reporters of cell quantification: Comparison with other cell quantification methods. *Molecules* (Basel, Switzerland), **26**, 5515.
Ma C, Gu C, Lian P, Wazir J, Lu R, Ruan B, Wei L, Li L, Pu W, Peng Z, Wang W, Zong Y, Huang Z, Wang H, Lu Y, Su Z. 2023. Sulforaphane alleviates psoriasis by enhancing antioxidant defense through KEAP1-NRF2 Pathway activation and attenuating inflammatory signaling. *Cell Death & Disease*, **14**, 768.
Migita H, Morser J, Kawai K. 2004. Rev-erbalpha upregulates NF-kappaB-responsive genes in vascular smooth muscle cells. *FEBS Letters*, **561**, 69–74.
Nestle M. 1998. Broccoli sprouts in cancer prevention. *Nutrition Reviews*, **56**, 127–130.
Al Olayan E M, Aloufi A S, AlAmri O D, El-Habit O H, Abdel Moneim Ahmed E. 2020. Protocatechuic acid mitigates cadmium-induced neurotoxicity in rats: Role of oxidative stress, inflammation and apoptosis. *Science of The Total Environment*, **23**, 137969.
Perissi V, Jepsen K, Glass C K, Rosenfeld M G. 2010. Deconstructing repression: Evolving models of co-repressor action. *Nature Reviews Genetics*, **1**, 109–123.
van der Pol A, van Gilst W H, Voors A A, and van der Meer P. 2019. Treating oxidative stress in heart failure: Past, present and future. *European Journal of Heart Failure*, **21**, 425–435.
Puchalska P, Crawford P A. 2021. Metabolic and signaling roles of ketone bodies in health and disease. *Annual Review of Nutrition*, **41**, 49–77.
Rao Z X, Tokach M D, Woodworth J C, DeRouchey J M, Goodband R D, Gebhardt J T. 2023. Effects of various feed additives on finishing pig growth performance and carcass characteristics: A review. *Animals* (Basel), **13**, 200.
Saha S, Buttari B, Panieri E, Profumo E, Saso L. 2020. An overview of Nrf2 signaling pathway and its role in inflammation. *Molecules*, **25**, 5474.
Sajadimajd S, Khazaei M. 2018. Oxidative stress and cancer: The role of Nrf2. *Current Cancer Drug Targets*, **18**, 538–557.
Saleh D O, Mansour D F, Hashad I M, Bakeer R M. 2019. Effects of sulforaphane on D-galactose-induced liver aging in rats: Role of keap-1/nrf-2 pathway. *European Journal of Pharmacology*, **855**, 40–49.
Sherman B T, Hao M, Qiu J, Jiao X, Baseler M W, Lane H C, Imamichi T, Chang W. 2022. DAVID: A web server for functional enrichment analysis and functional annotation of gene lists (2021 update). *Nucleic Acids Research*, **50**, W216–W221.
Socała K, Nieoczym D, Kowalczuk-Vasilev E, Wyska E, Wlaź P. 2017. Increased seizure susceptibility and other toxicity symptoms following acute sulforaphane treatment in mice. *Toxicology and Applied Pharmacology*, **32**, 643–653.
Thermo Fisher Scientific Inc. 2016. TRIzol™ Reagent User Guide. Pub. No. MAN0001271 Rev. D. [2023-6-3] https://assets.thermofisher.cn/TFS-Assets/LSG/manuals/trizol_reagent.pdf
Tian Y, Wu Y, Ni B. 2015. Signaling pathways and epigenetic regulations in the control of RORγt expression in T Helper 17 cells. *International Reviews of Immunology*, **34**, 305–317.
Tossetta G, Marzioni D. 2022. Natural and synthetic compounds in ovarian cancer: A focus on NRF2/KEAP1 pathway. *Pharmacological Research*, **183**, 106365.
Wang H, Wang B, Wei J, Zheng Z, Su J, Bian C, Xin Y, Jiang X. 2022. Sulforaphane regulates Nrf2-mediated antioxidant activity and downregulates TGF-β1/Smad pathways to prevent radiation-induced muscle fibrosis. *Life Sciences*, **311**, 121197.
Wolter B F, Ellis M, Corrigan B P, DeDecker J M, Curtis S E, Parr E

N, Webel D M. 2003. Impact of early postweaning growth rate as affected by diet complexity and space allocation on subsequent growth performance of pigs in a wean-to-finish production system. *Journal of Animal Science*, **81**, 353–359.

Wu Y K, Ren Z N, Zhu S L, Wu Y Z, Wang G, Zhang H, Chen W, He Z, Ye X L, Zhai Q X. 2022. Sulforaphane ameliorates non-alcoholic fatty liver disease in mice by promoting FGF21/FGFR1 signaling pathway. *Acta Pharmacologica Sinica*, **43**, 1473–1483.

Xu Y, Huang X, Huangfu B, Hu Y, Xu J, Gao R, Huang K, He X. 2023. Sulforaphane ameliorates nonalcoholic fatty liver disease induced by high-fat and high-fructose diet *via* LPS/TLR4 in the gut-liver axis. *Nutrients*, **15**, 743.

Yagishita Y, Fahey J W, Dinkova-Kostova A T, Kensler T W. 2019. Broccoli or sulforaphane: is it the source or dose that matters? *Molecules*, **24**, 3593.

Yang G, Wright C J, Hinson M D, Fernando A P, Sengupta S, Biswas C, La P, Dennery P A. 2014. Oxidative stress and inflammation modulate Rev-erbα signaling in the neonatal lung and affect circadian rhythmicity. *Antioxidants & Redox Signaling*, **21**, 17–32.

Yi T, Li X, Wang E, Zhang Y, Fu Y, Li J, Jiang T. 2018. Activation of the nuclear erythroid 2-related factor 2 antioxidant responsive element (Nrf2-ARE) signaling pathway alleviates acute graft-versus-host disease by reducing oxidative stress and inhibiting infiltration of inflammatory cells in an allogeneic stem cell transplantation mouse model. *Medical Science Monitor*, **24**, 5973–5979.

Zaghlool S S, Abdelaal N, El-Shoura E A M, Mahmoud N I, Ahmed Y M. 2023. Restoring glomerular filtration rate by sulforaphane modulates ERK1/2/JNK/p38MAPK, IRF3/iNOS, Nrf2/HO-1 signaling pathways against folic acid-induced acute renal injury in rats. *International Immunopharmacology*, **123**, 110777.

Zhang D, Tang Z, Huang H, Zhou G, Cui C, Weng Y, Liu W, Kim S, Lee S, Perez-Neut M, Ding J, Czyz D, Hu R, Ye Z, He M, Zheng Y G, Shuman H A, Dai L, Ren B, Roeder R G, Becker L, and Zhao Y. 2019. Metabolic regulation of gene expression by histone lactylation. *Nature*, **574**, 575–580.

Zhang H, Tang K, Ma J, Zhou L, Liu J, Zeng L, Zhu L, Xu P, Chen J, Wei K, Liang X, Lv J, Xie J, Liu Y, Wan Y, Huang B. 2020. Ketogenesis-generated β-hydroxybutyrate is an epigenetic regulator of CD8(+) T-cell memory development. *Nature Cell Biology*, **22**, 18–25.

Zhang S. 2023. From challenge to opportunity: Addressing oxidative stress in animal husbandry. *Antioxidants* (Basel), **12**, 1543.

Zhang Y Q, Shi C X, Zhang D M, Zhang L Y, Wang L W, Gong Z J. 2023. Sulforaphane, an NRF2 agonist, alleviates ferroptosis in acute liver failure by regulating HDAC6 activity. *Journal of Integrative Medicine*, **21**, 464–473.

Zhang Y, Wu Q, Liu J, Zhang Z, Ma X, Zhang Y, Zhu J, Thring R W, Wu M, Gao Y, Tong H. 2022. Sulforaphane alleviates high fat diet-induced insulin resistance *via* AMPK/Nrf2/GPx4 axis. *Biomedicine & Pharmacotherapy*, **152**, 113273.

Zhou T, Cheng Xi, He Y, Xie Y, Xu F, Xu Y, Huang W. 2022. Function and mechanism of histone β-hydroxybutyrylation in health and disease. *Frontiers in Immunology*, **13**, 981285.

Managing Editor Yanyan Sun